Synthesis, Photophysics, and Electrochemistry of Ruthenium(II) Polypyridine Complexes with Crown Ether Pendants

Vivian Wing-Wah Yam* and Vicky Wing-Man Lee

Department of Chemistry, The University of Hong Kong, Pokfulam Road, Hong Kong

Fu Ke and Kam-Wing Michael Siu

National Research Council of Canada, Institute for National Measurement Standards, M-12, Montreal Road, Ottawa, Ontario, Canada K1A 0R6

Received November 20, 1996[⊗]

A series of ruthenium(II) polypyridine complexes with a crown ether-containing ligand dipyrido[3,2-*a*:2′,3′-*c*]-phenazo-15-crown-5 (dppzc) have been synthesized and characterized and their photophysics and electrochemistry studied. The photoredox reactivities of $[Ru(bpy)_2(dppzc)]^{2+}$ have also been investigated by Stern−Volmer quenching experiments and nanosecond transient absorption spectroscopic studies. The cation-binding properties of these ruthenium(II) polypyridine complexes have also been studied by electronic absorption spectroscopy and cyclic voltammetry and confirmed by electrospray ionization mass spectrometry.

Introduction

The field of host−guest or supramolecular chemistry has continued to develop since the pioneering work of Pedersen,[1] Lehn,[2] and Cram[3] on the synthetic macrocyclic and macropolycyclic host systems such as the crown ethers, cryptands, and spherands. Design and synthesis of organic host molecules which could accommodate selectively a metal ion at its coordination site/cavity and undergo a concurrent color or redox change have been considered as a worthwhile subject in host−guest chemistry. Recently, increasing attention was paid on the design of inorganic hosts[4] with the awareness of the interesting photochemical and photophysical properties involved in the MLCT state of many inorganic systems. However, most of these studies focus on the synthesis and preliminary changes that occur upon cation binding, with relatively few systems subjected to intensive binding studies.[5,6]

As an extension of our previous works on transition metal complexes with crown ether pendants,[5,6] herein are reported the syntheses of a series of ruthenium(II) polypyridine complexes with crown ether pendants. The photophysics, photochemistry, and electrochemistry, as well as binding studies, are described.

Experimental Section

Ruthenium trichloride was obtained from Johnson-Matthey Chemical Co. 2,2′-Bipyridine (bpy) and 1,10-phenanthroline (phen) were obtained from Aldrich Chemical Co. 4,4′-Di-*tert*-butyl-2,2′-bipyridine (4,4′-^{t}Bu$_2$bpy),[7] 1,10-phenanthroline-5,6-dione (phen-dione),[8] benzo-15-crown-5, *o*-diaminobenzo-15-crown-5,[9,10] dipyrido[3,2-*a*:2′,3′-*c*]phenazine (dppz),[11,12] $[Ru(bpy)_2(dppz)]^{2+}$,[11] *cis*-$[Ru(bpy)_2Cl_2]$, *cis*-$[Ru(4,4'$-^{t}Bu$_2$bpy$)_2Cl_2]$, and *cis*-$[Ru(phen)_2Cl_2]$[13] were synthesized according to literature procedures. All other reagents were of analytical grade and were used as received.

Synthesis of Ruthenium(II)−dppzc Complexes. Dipyrido[3,2-*a*:2′,3′-*c*]phenazo-15-crown-5 (dppzc). The synthetic procedure was similar to that for dppz.[11,12] A mixture of *o*-diaminobenzo-15-crown-5 (298 mg, 1 mmol) and 1,10-phenanthroline-5,6-dione (210 mg, 1 mmol) was kept at reflux in 15 mL of ethanol for 24 h. The green suspension gradually turned brown. After cooling of the suspension to room temperature, the brown precipitate was collected by filtration. The brown residue obtained was then recrystallized with dichloromethane−ethanol. Yield: 260 mg, 55%. EI-MS: *m/z* 472. ^{1}H NMR (300 MHz, $CDCl_3$, 298 K, relative to Me_4Si): δ 3.84 (m, 8H, $-OCH_2-$), 4.06 (t, 4H, $-OCH_2-$), 4.40 (t, 4H, $-OCH_2-$), 7.51 (s, 2H, aryl protons of dppzc), 7.78 (dd, 2H, aryl protons of dppzc), 9.25 (dd, 2H, aryl protons of dppzc), 9.59 (dd, 2H, aryl protons of dppzc).

$[Ru(bpy)_2(dppzc)](PF_6)_2$ (1). A 52 mg (0.10 mmol) amount of *cis*-$[Ru(bpy)_2Cl_2]\cdot 2H_2O$ and 51 mg (0.20 mmol) of AgOTf were suspended in 25 mL of N_2-deaerated acetone. The mixture was stirred magnetically for 3 h and filtered by gravity. To the clear red solution was added 1.5 equiv of dppzc (70 mg, 0.15 mmol). The solution was deaerated by N_2 bubbling and then refluxed for 12 h with vigorous stirring using a magnetic stirrer. The reddish orange solution was then evaporated to dryness. The orange residue was then extracted with ethanol, the extract was filtered, and a solid was precipitated with aqueous NH_4PF_6. The precipitate was collected by filtration and washed with diethyl ether to remove any unreacted dppzc ligand. The crude product was recrystallized from acetonitrile−diethyl ether to give pure reddish orange crystals. Yield: 55 mg, 47%. Positive ion FAB-MS: *m/z* 1030 $\{M(PF_6)\}^+$, 885 $\{M\}^+$, 699 $\{M - bpy\}^+$. ^{1}H NMR (300

[⊗] Abstract published in *Advance ACS Abstracts,* April 15, 1997.

(1) (a) Pedersen, C. J. *J. Am. Chem. Soc.* **1967**, *89*, 8017. (b) Pedersen, C. J. *Angew. Chem., Int. Ed. Engl.* **1988**, *27*, 1021.
(2) (a) Lehn, J. M. *Struct. Bonding (Berlin)* **1973**, *16*, 1. (b) Lehn, J. M. *Angew. Chem., Int. Ed. Engl.* **1988**, *27*, 59.
(3) Cram, D. J. *Angew. Chem., Int. Ed. Engl.* **1988**, *27*, 1009.
(4) (a) Van Veggel, F. C. J. M.; Verboom, W.; Reinhoudt, D. N. *Chem. Rev.* **1994**, *94*, 279. (b) Beer, P. D. *Adv. Inorg. Chem.* **1992**, *39*, 79. (c) Beer, P. D.; Kocian, O.; Mortimer, R. J.; Ridgway, C. *J. Chem. Soc., Dalton Trans.* **1993**, 2629.
(5) Yam, V. W. W.; Lo, K. K. W.; Cheung, K. K. *Inorg. Chem.* **1995**, *34*, 4013.
(6) Yam, V. W. W.; Wong, K. M. C.; Lee, V. W. M.; Lo, K. K. W.; Cheung, K. K. *Organometallics* **1995**, *14*, 4034.
(7) Sasse, W. H. F. *Organic Syntheses*; Wiley: New York, 1973; Collect. Vol. V, p 102.
(8) Hiort, C.; Lincoln, P.; Norden, B. *J. Am. Chem. Soc.* **1993**, *115*, 3448.
(9) Ungaro, R.; Haj, E. E.; Smid, J. *J. Am. Chem. Soc.* **1976**, *98*, 5198.
(10) Pacey, G. E.; Wu, Y. P.; Bubnis, B. P. *Synth. Commun.* **1981**, *11*, 323.
(11) Amouyal, E.; Homsi, A.; Chambron, J. C.; Sauvage, J. P. *J. Chem. Soc., Dalton Trans.* **1990**, 1841.
(12) Yamada, M.; Tanake, Y.; Yoshimoto, Y.; Kuroda, S.; Shimao, I. *Bull. Chem. Soc. Jpn.* **1992**, *65*, 1006.
(13) Sullivan, B. P.; Salmon, D. J.; Meyer, T. J. *Inorg. Chem.* **1978**, *17*, 3334.

S0020-1669(96)01400-0 CCC: $14.00

MHz, CD_3CN, 298 K, relative to Me_4Si): δ 3.60 (m, 8H, $-OCH_2-$), 3.90 (m, 4H, $-OCH_2-$), 4.40 (m, 4H, $-OCH_2-$), 7.25 (t, 2H, bpy), 7.45 (t, 2H, bpy), 7.50 (s, 2H, aryl protons of dppzc), 7.58 (d, 2H, bpy), 7.70 (d, 2H, bpy), 7.85 (t, 2H, aryl protons of dppzc), 8.02 (t, 2H, bpy), 8.10 (t, 2H, bpy), 8.23 (d, 2H, aryl protons of dppzc), 8.50 (dd, 4H, bpy), 9.50 (dd, 2H, aryl protons of dppzc). Anal. Calcd for $[Ru(bpy)_2(dppzc)](OTf)_2 \cdot 2H_2O$: C, 47.26; H, 3.64; N, 9.28. Found: C, 47.52; H, 3.74; N, 9.13.

$[Ru(4,4'\text{-}^tBu_2bpy)_2(dppzc)](PF_6)_2$ (2). The procedure was similar to that of **1** except *cis*-$[Ru(4,4'\text{-}^tBu_2bpy)_2Cl_2] \cdot H_2O$ (64 mg, 0.1 mmol) was used instead of *cis*-$[Ru(bpy)_2Cl_2] \cdot 2H_2O$ to give orange crystals of **2**. Yield: 70 mg, 50%. Positive ion FAB-MS: *m/z* 1254 $\{M(PF_6)\}^+$, 1109 $\{M\}^+$. ^1H NMR (300 MHz, CD_3CN, 298 K, relative to Me_4Si): δ 1.31 (s, 18H, ^{t}Bu), 1.43 (s, 18H, ^{t}Bu), 3.67−3.75 (m, 8H, $-OCH_2-$), 3.95 (m, 4H, $-OCH_2-$), 4.40 (m, 4H, $-OCH_2-$), 7.23 (dd, 2H, 4,4′-^{t}Bu$_2$bpy), 7.47 (dd, 2H, 4,4′-^{t}Bu$_2$bpy), 7.56 (d, 2H, 4,4′-^{t}Bu$_2$bpy), 7.58 (s, 2H, aryl protons of dppzc), 7.70 (d, 2H, 4,4′-^{t}Bu$_2$bpy), 7.87 (dd, 2H, aryl protons of dppzc), 8.49 (d, 2H, 4,4′-^{t}Bu$_2$bpy), 8.09 (dd, 2H, aryl protons of dppzc), 8.53 (d, 2H, 4,4′-^{t}Bu$_2$bpy), 9.55 (dd, 2H, aryl protons of dppzc). Anal. Calcd for $[Ru(4,4'\text{-}^tBu_2bpy)_2(dppzc)](PF_6)_2$: C, 53.03; H, 5.45; N, 7.98. Found: C, 53.11; H, 5.66; N, 8.03.

$[Ru(phen)_2(dppzc)](PF_6)_2$ (3). The procedure was similar to that of **1** except *cis*-$[Ru(phen)_2Cl_2] \cdot H_2O$ (57 mg, 0.1 mmol) was used instead of *cis*-$[Ru(bpy)_2Cl_2] \cdot 2H_2O$ to give orange crystals of **3**. Yield: 50 mg, 41%. Positive ion FAB-MS: *m/z* 1078 $\{M(PF_6)\}^+$, 933 $\{M\}^+$. ^1H NMR (300 MHz, CD_3CN, 298 K, relative to Me_4Si): δ 3.67−3.72 (m, 8H, $-OCH_2-$), 3.91 (m, 4H, $-OCH_2-$), 4.35 (m, 4H, $-OCH_2-$), 7.51 (s, 2H, aryl protons of dppzc), 7.60−7.80 (m, 6H, phen), 7.82 (t, 2H, aryl protons of dppzc), 8.05 (d, 2H, phen), 8.10 (d, 2H, phen), 8.23 (d, 2H, aryl protons of dppzc), 8.30 (s, 2H, phen), 8.65 (dd, 4H, phen), 9.50 (d, 2H, aryl protons of dppzc). Anal. Calcd for $[Ru(phen)_2(dppzc)](PF_6)_2$: C, 53.47; H, 3.59; N, 9.97. Found: C, 53.52; H, 3.72; N, 9.77.

$[Ru(dppzc)_3](PF_6)_2$ (4). An ethanolic solution of $RuCl_3 \cdot H_2O$ (45 mg, 0.19 mmol) was added dropwise to a warm acetone (7 mL) solution of dppzc (302 mg, 0.64 mmol) and refluxed for 24 h. After reflux, the bright red solution was concentrated to one-third of the initial volume and then H_2O (10 mL) was added. The solution was filtered to remove any unreacted dppzc. Addition of excess NH_4PF_6 to the filtrate precipitated a reddish orange flocculent solid. The product was subsequently recrystallized from acetone−diethyl ether to give deep reddish orange crystals. Yield: 115 mg, 33%. Positive ion FAB-MS: *m/z* 1517 $\{M\}^+$. ^1H NMR (300 MHz, CD_3CN, 298 K, relative to Me_4Si): δ 3.64−3.91 (m, 8H, $-OCH_2-$), 4.36 (t, 4H, $-OCH_2-$), 4.91 (t, 4H, $-OCH_2-$), 7.55 (s, 2H, aryl protons of dppzc), 7.78 (dd, 2H, aryl protons of dppzc), 8.25 (dd, 2H, aryl protons of dppzc), 9.54 (d, 2H, aryl protons of dppzc). Anal. Calcd for $[Ru(dppzc)_3](PF_6)_2 \cdot 5H_2O$: C, 49.35; H, 4.35; N, 8.85. Found: C, 49.38; H, 4.32; N, 8.61.

Physical Measurements and Instrumentation. UV/vis spectra were obtained on a Hewlett-Packard 8452A diode array spectrophotometer, and steady-state excitation and emission spectra, on a Spex Fluorolog 111 spectrofluorometer. Low-temperature (77 K) spectra were recorded by using an optical Dewar sample holder. ^1H NMR spectra were recorded on a Bruker DPX-300 Fourier-transform NMR spectrometer with chemical shifts reported relative to tetramethylsilane. Positive ion FAB mass spectra were recorded on a Finnigan MAT95 mass spectrometer. Elemental analyses of the new complexes were performed by Butterworth Laboratories Ltd.

Emission lifetime measurements were performed using a conventional laser system. The excitation source was the 355-nm output (third harmonic) of a Quanta-Ray Q-switched GCR-150-10 pulsed Nd-YAG laser. Luminescence decay signals were recorded on a Tektronix Model TDS 620A digital oscilloscope and analyzed using a program for exponential fits. All solutions for photophysical studies were prepared under vacuum in a 10-cm^3 round-bottomed flask equipped with a side-arm 1-cm fluorescence cuvette and sealed from the atmosphere with a Kontes quick-release Teflon stopper. Solutions were rigorously degassed with no fewer than four freeze−pump−thaw cycles.

Cyclic voltammetric measurements were carried out with a PAR Model 175 universal programmer and Model 173 potentiostat. Cyclic voltammograms were recorded with a Kipp & Zonen BD90 X-Y recorder at scan rates 50−500 mV s^{-1}. The electrolytic cell used was a conventional two-compartment cell. The reference electrode is the $Ag/AgNO_3$ (0.1 M in acetonitrile) electrode with a vycor glass interfacing the working electrode compartment. Electrochemical studies were performed in nonaqueous medium (0.1 M NBu_4PF_6 in acetonitrile) with the glassy carbon (Atomergic Chemetal V25) electrode as working electrode and a piece of platinum gauze as counter electrode which is separated from the working electrode by a sintered glass frit. The ferrocenium/ferrocene couple ($FeCp_2^{+/0}$) was used as the internal reference in nonaqueous media.

Table 1. Electrochemical Data for Complexes **1**−**4** and Their Uncrowned Analogues

complex	redn $E_{1/2}$ vs SCE/V ($E_{1/2}$ in Na^+)[a]	oxidn $E_{1/2}$ vs SCE/V ($E_{1/2}$ in Na^+)[a]
1	−1.20 (−1.11), −1.46 (−1.46), −1.67 (−1.66)	1.33 (1.33)
2	−1.20 (−1.13), −1.55, −1.78	1.21 (1.20)
3	−1.18 (−1.08)	1.28 (1.29)
4	−1.15 (−1.07)	1.33 (1.33)
$[Ru(bpy)_2(dppz)]^{2+}$	−1.02 (1.02), −1.46, −1.69	1.34 (1.33)
$[Ru(dppz)_3]^{2+}$	−1.00[b]	1.37[b]

[a] $E_{1/2}$ values in parentheses are potential values in the presence of $NaClO_4$ in acetonitrile (0.1 M NBu_4PF_6). [b] From ref 14.

The electronic absorption spectral titration for binding constant determination was performed with a Hewlett-Packard 8452A diode array spectrophotometer at 25 °C controlled by the Lauda RM6 compact low-temperature thermostat. Supporting electrolyte (0.1 M NBu_4PF_6) was added to maintain the ionic strength of the sample solution constant during the titration in order to avoid any changes arising from a change in the ionic strength of the medium. This is especially important for MLCT transitions which are usually rather sensitive to the nature of the solution medium.

Electrospray mass spectrometric experiments were performed on a SCIEX TAGA Model 6000E triple quadrupole mass spectrometer, which has an upper mass limit of *m/z* ∼ 1400, at the Institute for National Measurement Standards, National Research Council of Canada, Ottawa, Canada. The details of which were described in the Supporting Information.

Results and Discussion

The dipyrido[3,2-*a*:2′,3′-*c*]phenazo-15-crown-5 (dppzc) ligand, which consists of a dppz ligand with polyether substituents, was

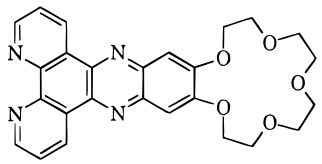

dppzc

synthesized by the reaction of *o*-diaminobenzo-15-crown-5 and 1,10-phenanthroline-5,6-dione in alcohol, modified from the procedure for dppz synthesis.[11,12] All the newly synthesized complexes have been characterized by positive ion FAB-MS and ^1H NMR spectroscopy and gave satisfactory elemental analyses.

Electrochemical Properties. The electrochemical data for the ruthenium(II)−dppzc complexes in acetonitrile are summarized in Table 1. The cyclic voltammogram of **1** is shown in Figure 1 as a representative of the series $[Ru(N\frown N)_2(dppzc)]^{2+}$. Three quasi-reversible reduction couples and one reversible oxidation couple were observed. The first reduction, which is present in all complexes **1**−**4**, is assigned as the dppzc-centered reduction, while the other two reductions at more negative potentials, which occur only in complexes **1** and **2**, are assigned as derived from the sequential one-electron reduction of the bipyridyl ligand. The occurrence of these two

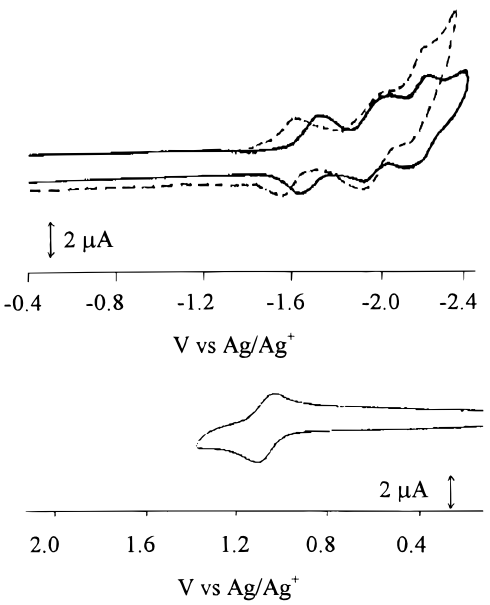

Figure 1. Cyclic voltammograms of complex **1** in acetonitrile (0.1 mol dm^{-3} NBu_4PF_6) in the absence (solid line) and in the presence (dashed line) of $NaClO_4$. Scan rate = 100 mV s^{-1}. $E_{1/2}(FeCp_2^{+/0})$ = +0.1 V vs Ag/Ag^+.

couples at more negative potential in **2** than **1** is in line with the reduced ease of reduction of the more electron-rich ^{t}Bu$_2$-bpy ligand. Similar reduction potentials for the successive reduction of the bipyridyl ligands as in **1** were observed in the analogous $[Ru(bpy)_2(dppz)]^{2+}$. The cyclic voltammogram of the homoleptic complex **4** showed only one quasi-reversible reduction couple at −1.15 V vs SCE, corresponding to the reduction of the dppzc ligand. The more negative reduction potential of **4** compared to that of the uncrowned $[Ru(dppz)_3]^{2+}$, which occurs at −1.00 V vs SCE,[14] is in line with the reduced ease of reduction of the dppzc ligand with electron-donating polyether substituents. Similarly, the dppzc-centered reduction in **1** occurs at more negative potential than the corresponding dppz-centered reduction in $[Ru(bpy)_2(dppz)]^{2+}$.

The oxidation couples occurred in the range typical of $Ru^{3+/2+}$ couples and were assigned as ruthenium metal-based oxidation. The metal-based oxidation couples occurred at fairly similar potentials and appeared to be relatively insensitive to the nature of the dppz-type ligand. For example, the oxidation couple of $[Ru(dppz)_3]^{2+}$ and **4** occurred at +1.37 [14] and +1.33 V vs SCE, respectively, despite the presence of electron-donating polyether moieties attached to the phenazine ring in dppzc. Furthermore, complexes with ligands containing lower-lying π^* orbitals are expected to show oxidation couples at more positive potentials as the $d\pi(Ru)-\pi^*(L)$ interaction would preferentially stabilize the lower oxidation state. The dppzc ligand is expected to have a more conjugated system and therefore a lower π^* energy than bpy, as reflected by its less negative ligand-centered reduction potential than the bpy counterpart. However, to our surprise, both **4** and **1** have $E_{1/2}[Ru^{3+/2+}]$ values at +1.33 V vs SCE, which are similar to the value of +1.29 V vs SCE for the ruthenium-based oxidation in $[Ru(bpy)_3]^{2+}$. This relative insensitivity of the $E_{1/2}[Ru^{3+/2+}]$ value is consistent with previous studies on $[Ru(bpy)_2(dppz)]^{2+}$.[14] The π-accepting site in dppzc is likely to be localized on the phenazine portion of the molecule which is only weakly coupled electronically to the ruthenium metal center. On the other hand, the oxidation couple of **2** occurs at less positive potential than that of **1**, in line with the increased ease of oxidation of **2** with the more electron-donating ^{t}Bu$_2$bpy ligand.

The cyclic voltammogram of **1** in the presence and absence of Na^+ ions is shown in Figure 1. Upon addition of Na^+ ions, a 90-mV anodic shift in the dppzc-based reduction was observed while there were no obvious changes in the other couples. The anodic shift observed may probably be attributed to the inclusion of the cation in the crown cavity, which may be viewed as an electron-withdrawing group, as such shift was absent in similar studies with the uncrowned analogue $[Ru(bpy)_2(dppz)]^{2+}$. Anodic shifts of 70 and 30 mV were observed upon addition of Li^+ and K^+, respectively. This suggests that the effect of Na^+ and Li^+ are similar while that of K^+ is smaller. Control experiments using the uncrowned ruthenium(II) complexes showed no shifts in the redox couples upon addition of cations, indicative of the authentic binding nature of the crown analogues and the elimination of the possibility of an ionic effect. Similarly, the effect of counteranions has been shown to be minimal as variation of the counteranion of the alkali metal salts did not show any significant effect on the shift of the potential.

Inspection of Table 1 revealed that comparable effects of cation inclusion also occurred for complexes **2**−**4**. The anodic shift in the first reduction wave upon addition of Na^+ ions to solutions of complexes **2**−**4** are 70, 95 and 80 mV, respectively. This suggests that the spectator ligands do not have a significant influence on the binding activity of the dppzc ligand. In the case of **4** that contains three crown pendants, the Na^+ ion inclusion did not show conspicuous effect on the ruthenium-based oxidation. This is also consistent with the poor communication between the phenazocrown unit and the ruthenium metal center.

Electronic Absorption and Photophysical Properties. The electronic absorption and photophysical data for complexes **1**−**4** are summarized in Table 2. The electronic absorption spectra are dominated by an intense absorption at *ca*. 290 nm, which is assigned as a ligand-centered transition as commonly observed in polypyridine complexes. Two lower energy absorption bands are observed in the visible region of the spectra. With reference to previous spectroscopic work on related systems,[11,14,15] the absorption band at *ca*. 370−400 nm is assigned as the $\pi \rightarrow \pi^*$(dppzc) transition, while the lowest energy absorption band at *ca*. 440−456 nm is assigned as an admixture of a higher energy $d\pi(Ru) \rightarrow \pi^*$(bpy or phen) MLCT and a lower energy $d\pi(Ru) \rightarrow \pi^*$(dppzc) MLCT transition. Similar assignments for the related $[Ru(Me_2bpy)_2(dppz)]^{2+}$ complex have been supported by resonance Raman spectroscopic studies.[15] The similarity in the MLCT absorption energies between complexes **1**−**4** and $[Ru(bpy)_3]^{2+}$ may be a consequence of the bichromophoric character of these complexes as reported by Ackermann and Interrante.[14]

Similar to most $[Ru(N^{\frown}N)_3]^{2+}$ complexes, both solid-state samples and acetonitrile solutions of the complexes were found to be strongly luminescent with emission maxima at *ca*. 600−640 nm at room temperature upon excitation at $\lambda > 350$ nm. The emission is derived from the lowest triplet MLCT [$d\pi(Ru) \rightarrow \pi^*$(dppzc)] state which is typical for ruthenium(II) polypyridine systems. The emission energies of the complexes follow the order **2** < **1** ≤ **3** ≤ **4**, in line with the order of the $d\pi$ orbital energy of ruthenium(II) which is in the reverse order, **2** > **1** ≥ **3** > **4**.

Addition of a variety of cations to acetonitrile solutions of this class of complexes, which unlike the system reported by Beer,[4c] gave rise to a small red shift in the emission maxima

(14) Ackermann, M. N.; Interrante, L. V. *Inorg. Chem.* **1984**, *23*, 3904.

(15) Schoonover, J. R.; Bates, W. D.; Meyer, T. J. *Inorg. Chem.* **1995**, *34*, 6421.

Table 2. Electronic Absorption and Photophysical Data for Complexes **1**−**4** in Acetonitrile at 298 K

complex	salt added	λ_{abs}/nm ($10^{-4}\epsilon$/dm^3 mol^{-1} cm^{-1})	emission max/nm	τ_o/μs
1	no salt	290 (9.63), 394 (3.39), 452 (2.20)	605	1.0
	0.1 M Bu_4NPF_6	290 (9.65), 394 (3.30), 452 (2.12)	605	
	0.1 M $NaClO_4$	288 (10.4), 388 (3.50), 452 (2.03)	611	
	0.1 M $LiClO_4$	288 (10.5), 388 (3.50), 452 (2.01)	611	
	0.1 M KPF_6	288 (10.4), 390 (3.56), 452 (2.15)	609	
2	no salt	290 (8.10), 376 (2.11), 396 (3.04), 442 (1.65)	624	1.4
	0.1 M Bu_4NPF_6	288 (8.93), 378 (2.13), 396 (2.85), 440 (1.42)	624	
	0.1 M $NaClO_4$	288 (9.62), 372 (2.12), 390 (3.03), 442 (1.57)	632	
	0.1 M $LiClO_4$	288 (10.1), 370 (2.14), 390 (3.08), 442 (1.60)	633	
	0.1 M KPF_6	288 (9.58), 374 (2.27), 392 (3.15), 440 (1.69)	627	
3	no salt	294 (6.74), 396 (4.00), 450 (2.31)	600	0.93
	0.1 M Bu_4NPF_6	295 (6.89), 394 (3.88), 450 (2.21)	600	
	0.1 M $NaClO_4$	288 (7.99), 388 (3.98), 450 (2.14)	606	
	0.1 M $LiClO_4$	288 (8.10), 388 (4.03), 450 (2.14)	605	
	0.1 M KPF_6	290 (7.82), 392 (4.10), 448 (2.66)	602	
4	no salt	300 (14.9), 378 (6.65), 396 (9.19), 456 (3.62)	593	0.75
	0.1 M Bu_4NPF_6	300 (14.8), 378 (6.59), 396 (9.10), 456 (3.57)	594	
	0.1 M $NaClO_4$	292 (16.4), 368 (6.05), 390 (9.36), 456 (3.13)	598	
	0.1 M $LiClO_4$	292 (17.4), 368 (6.18), 388 (9.48), 456 (3.12)	599	
	0.1 M KPF_6	294 (16.5), 374 (6.96), 392 (9.68), 456 (3.54)	597	

Table 3. Bimolecular Quenching Rate Constant Data for **1** by a Series of Pyridinium Acceptors at 298 K

quencher[a]	$E(A^+/A)$/V vs SCE[b]	k_q/dm^3 mol^{-1} s^{-1}
N,*N*′-dimethyl-4,4′-bipyridinium	−0.45	1.5×10^9
N-methyl-4-cyanopyridinium	−0.67	2.8×10^9
N-methyl-4-(methylcarboxy)pyridinium	−0.78	1.5×10^9
N-methyl-4-amidopyridinium	−0.93	9.8×10^7
N-ethyl-3-amidopyridinium	−1.14	7.5×10^7
N-ethylpyridinium	−1.36	3.8×10^6

[a] All pyridinium acceptors are hexafluorophosphates. [b] From ref 17.

Table 4. Bimolecular Quenching Rate Constant Data for **1** by a Series of Aromatic Amines at 298 K

quencher	$E(D^{\bullet+}/D)$/V vs SCE[a]	k_q/dm^3 mol^{-1} s^{-1}
N,*N*,*N*′,*N*′-tetramethyl-1,4-phenylenediamine	0.16	1.1×10^{10}
1,4-phenylenediamine	0.17	7.6×10^9
N,*N*,*N*′,*N*′-tetramethylbenzidine	0.32	1.1×10^9
3,3′-dimethylbenzidine	0.45	6.0×10^9
phenothiazine	0.53	6.0×10^9
1,4-anisidine	0.71	2.4×10^9
toluidine	0.78	5.1×10^8

[a] From ref 18.

and a slight increase in the emission intensity. It is likely that upon inclusion of cations which could be viewed as an electron-withdrawing group, the π^* of the dppzc ligand would be lowered and resulted in lower emission energy. The emission maxima of the complexes in the presence of different cations are summarized in Table 2. The increase in intensity may result from the increased energy difference between the ^{3}MLCT and ^{3}LF states upon cation inclusion, which reduced the rate of the thermally activated ^{3}MLCT to ^{3}LF state transition. Similar findings have been observed in the protonation reaction of the ruthenium(II)−terpyridine system where the energy gap law is not obeyed.[16] An alternative rationale for the enhanced emission intensity could be ascribed to the blocking of the photo-induced electron transfer quenching mechanism upon cation inclusion since the unbound crown could be viewed as a dialkoxybenzene moiety which is known to be a good electron donor.

Photoredox Studies. The photoredox reactivities of $[Ru(bpy)_2(dppzc)]^{2+}$ have also been explored. The bimolecular quenching rate constant data of $[Ru(bpy)_2(dppzc)]^{2+*}$ by a series of aromatic amines and pyridinium salts[17,18] in acetonitrile (0.1 M NBu_4PF_6) are summarized in Tables 3 and 4, respectively. All the reactions obey the Stern−Volmer equation, $\tau_o/\tau = 1 + k_q\tau_o[Q]$ in the concentration range used. The dependence of the quenching rate constants on the reduction potential of the quenchers suggests that electron transfer is the predominant luminescence quenching mechanism of $[Ru(bpy)_2(dppzc)]^{2+*}$ by aromatic amines and pyridinium salts.

In order to establish the electron transfer nature of the quenching reaction, nanosecond transient absorption spectroscopy was employed. The transient absorption difference spectrum generated from the laser flash photolysis of an acetonitrile solution of $[Ru(bpy)_2(dppzc)]^{2+}$ (5×10^{-5} mol dm^{-3}) and methyl viologen hexafluorophosphate (MV^{2+}, 5 mmol dm^{-3}) with 0.1 mol dm^{-3} NBu_4PF_6 as supporting electrolyte shows an intense absorption at *ca.* 390 nm and a very broad band centered at *ca.* 600 nm, characteristic of absorptions for the reduced methyl viologen cation radical.[19] Besides, bleaching at *ca.* 425 nm is observed, probably as a consequence of the depletion of $[Ru(bpy)_2(dppzc)]^{2+}$ which absorbs strongly in the region. Similar reactions with triphenylamine (TPA) and *N*,*N*,*N*′,*N*′-tetramethylbenzidine (TMB) were performed. The production of the cation radicals of the quenchers TPA and TMB was verified by the generation of transient absorptions at *ca.* 600 nm for $TPA^{\bullet+}$ [20] and *ca.* 460 nm for $TMB^{\bullet+}$.[21] The electron transfer nature of the quenching mechanism is consistent with the prediction that energy transfer does not contribute to a significant extent since the triplet state energies of the quenchers are too high for energy transfer to be competitive with electron-transfer quenching.

Cation-Binding Studies. Upon addition of alkali metal cations to an acetonitrile solution of $[Ru(N\frown N)_2(dppzc)]^{2+}$, the absorption at *ca.* 380−394 nm would exhibit a blue shift in energy. The UV−visible absorption spectral traces upon sequential addition of sodium cations to a solution of $[Ru(bpy)_2(dppzc)]^{2+}$ are shown in Figure 2. These shifts were ascribed to the binding of the cations to the polyether cavity, as similar effects were absent for the uncrowned complex $[Ru(bpy)_2$-

(16) Barigelletti, F.; Flamigni, L.; Guardigli, M.; Sauvage, J.-P.; Collin, J.-P.; Sour, A. *Chem. Commun.* **1996**, 1329.
(17) Marshall, J. L.; Stobart, S. R.; Gray, H. B. *J. Am. Chem. Soc.* **1984**, *106*, 3027.
(18) Bock, C. R.; Connor, J. A.; Gutierrez, A. R.; Meyer, T. J.; Whitten, D. G.; Sullivan, B. P.; Nagle, J. K. *J. Am. Chem. Soc.* **1984**, *106*, 3027.
(19) Watanbe, T.; Honda, K. *J. Phy. Chem.* **1982**, *20*, 39.
(20) Shida, T.; Hamill, W. H. *J. Chem. Phys.* **1966**, *44*, 2369.
(21) Ohno, T.; Kato, S. *Bull. Chem. Soc. Jpn.* **1984**, *57*, 1528.

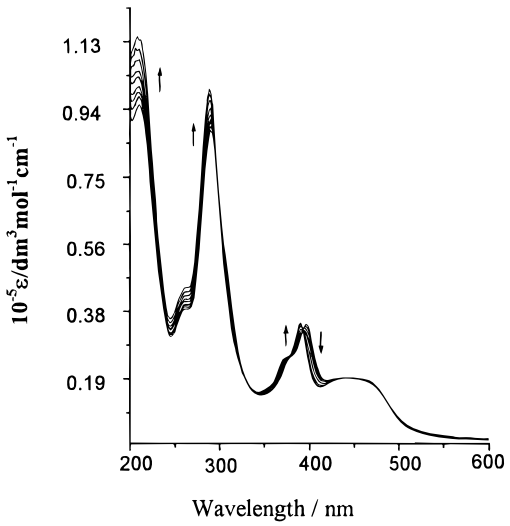

Figure 2. Electronic absorption spectral traces of **1** in acetonitrile upon addition of $NaClO_4$ at 298 K.

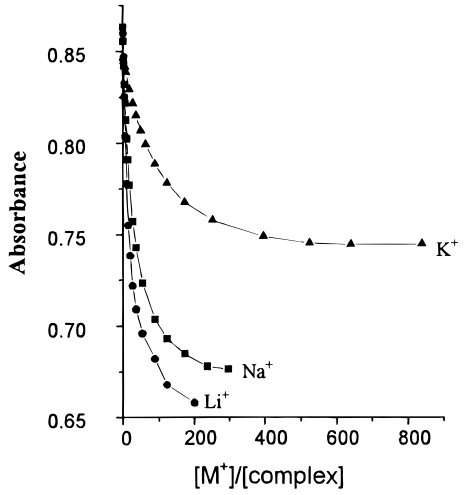

Figure 3. Electronic absorption titration curves for **1** with alkali metal cations in acetonitrile at 298 K. The absorbance was monitored at 410 nm.

(dppz)]$^{2+}$. The spectral changes were reversible upon addition of free 15-crown-5 or 18-crown-6 which has a higher affinity for the alkali metal cations relative to the [Ru(N⁀N)$_2$(dppzc)]$^{2+}$ complexes. Studies on the interaction between the complexes and the sodium cation were performed by following the spectral changes. Similar changes are observed upon addition of lithium and potassium cations.

Figure 3 shows a summary of the titration curves monitoring the changes in absorbance of an acetonitrile solution of complex **1** at 410 nm upon addition of sodium, potassium, and lithium salts. The curves show a gradual decrease in absorbance at 410 nm upon increasing the cation concentration, reaching saturation at higher cation concentrations. With such absorption information, the binding constants could be determined with the following equation:

$$\frac{A_o}{A_o - A} = \left(\frac{\epsilon_f}{\epsilon_f - \epsilon_b}\right)\left(1 + \frac{1}{K_s[M]}\right)$$

Here A_o is the absorbance in the absence of alkali metal ions, A is the absorbance of the solution mixture at an alkali metal cation concentration [M], ϵ_f and ϵ_b are the molar extinction coefficients of the host complex [Ru(N⁀N)$_2$(dppzc)]$^{2+}$ and the bound species [Ru(N⁀N)$_2$(dppzc)·Na]$^{3+}$, respectively, and K_s is the binding constant.

Table 5. Binding Constants of Complexes **1**−**4** with Alkali Metal Cations at 298 K[a]

		log K_s		
complex	medium	Na^+	K^+	Li^+
1	CH_3CN	3.08	2.28	3.45
	$(CH_3)_2CO$	2.31	2.13	1.64
	CH_3OH	1.42	*b*	*b*
2	CH_3CN	3.10	2.51	3.17
3	CH_3CN	2.97	2.48	3.35
4	CH_3CN	3.06	2.55	3.52

[a] The salts used were $NaClO_4$, KPF_6, and $LiClO_4$. [b] The binding constant cannot be determined with certainty.

Transforming the UV−vis spectral data into a plot of $A_o/(A_o - A)$ vs $[M^+]^{-1}$ gave a satisfactory straight line. From the plot of $A_o/(A_o - A)$ vs $[M]^{-1}$, the stability constant can be determined by the ratio of *y*-intercept/slope.[22] The calculated stability constants for the complexes are summarized in Table 5. Inspection of Table 5 reveals that the binding constants of sodium cations in acetonitrile for all the complexes studied are of similar values. The binding constants of the complexes toward lithium and potassium ions are also similar. This suggests that the spectator ligands would have negligible effects on the crown ligand and would not significantly alter the binding ability of the complexes to a noticeable extent. In the case of **4**, no further binding was observed and only one binding constant was obtained. This may be rationalized by the high positive charge developed after binding of the first cation, which renders further binding unfavorable.

Investigation of the effect of solvents on the binding activities was also carried out with three different solvents, acetonitrile, acetone, and methanol. The choice of solvents was limited by the solubility of the ruthenium(II)−crown complexes, the alkali metal salts, and the bound species.

In general, the binding constants of lithium, sodium, and potassium cations in different solvents are found to follow the order acetonitrile > acetone > methanol. It is likely that in methanol, which is the most polar among the three, the cations are already well solvated, or well stabilized, by the solvent molecules, seeking a binding site in the crown cavity is no longer a necessity to stabilize the cation, leading to the smallest binding constant. Solvent effects on cation binding have also been well documented for the simple crown compounds such as 15-crown-5 or benzo-15-crown-5. Frensdorf[23] noted that the binding constants, K_s, of cyclic polyethers for metal cations are 10^3 to 10^4 times larger in methanol than in water. The log K_s value for the interaction of Na^+ with benzo-15-crown-5 increases regularly with increasing weight percent of CH_3OH.[24] The enhancement of stability in methanol over that in water has been attributed primarily to an enthalpic effect.[24,25] On the other hand, the difference between the reaction entropies found in water and those found in methanol opposes this stability enhancement. Therefore, the variation of complexation by the crown complexes demonstrated here in several solvents of low to medium donor ability, such as acetonitrile and acetone, is likely to be a result of the compensating effect (enthalpy stabilized and entropy destabilized).[26]

(22) (a) Bourson, J.; Valeur, B. *J. Phys. Chem.* **1989**, *93*, 3871. (b) Frey-Forgues, S.; Le Bris, M. T.; Ginette, J. P.; Valeur, B. *J. Phys. Chem.* **1988**, *92*, 6233.
(23) Frensdorf, H. K. *J. Am. Chem. Soc.* **1971**, *93*, 600.
(24) Izatt, R. M.; Terry, R. E.; Nelson, D. P.; Chan, Y.; Eatough, D. J.; Bradshaw, J. S.; Hansen, L. D.; Christensen, J. J. *J. Am. Chem. Soc.* **1976**, *98*, 7626.
(25) Kauffmann, E.; Lehn, J. M.; Sauvage, J. P. *Helv. Chim. Acta*, **1976**, *59*, 1099.

The binding constants, or the stability constants, of the cation-bound complexes in acetonitrile studied are in the order $Li^+ > Na^+ > K^+$. This phenomenon is common for the typical 15-crown-5 compounds in acetonitrile.[27] This is consistent with the order of charge density of the cations: $Li^+ > Na^+ > K^+$. The exceptionally small size of the lithium cation inherits the highest charge density. The sodium cations of slightly lower charge density also acquired the binding constant of the same order as it is well-known that 15-crown-5 compounds have their hole size tailor-made for sodium cations. The small binding constant for the potassium cation is attributed to its large size, which makes it difficult to fit into the 15-crown-5, giving rise to the low stability of the bound species. The stability of the bound species can be increased with the formation of a sandwiched species which has two crowns sitting above and below the potassium cation like a sandwich. However, in the case of these ruthenium(II)−crown complexes with an overall positive charge of +2, the formation of the sandwiched species is not favored by the instability offered by the development of such highly charged sandwiches.

Unlike the case in acetonitrile, the binding selectivity of **1** in methanol was in the order of $Na^+ > K^+ > Li^+$. This observed trend concurs with the ESI mass spectrometric data which are summarized in Table 6. The identities of the ion clusters have been confirmed by matching the expanded spectra with the simulated isotope patterns. The relative intensity of the cation bound species in the ESI-mass spectrum in the order of $Na^+ > K^+ > Li^+$ only represents a preliminary comparison of binding selectivity toward a variety of cations, and quantitative correlation between the ionic species could not be established because of the difference in the desorption efficiencies of different charged species. In conclusion, both the ESI-mass spectrometric data and the electronic absorption titration results suggest that the selectivity of **2** toward alkali metal cations is in the order of $Na^+ > K^+ > Li^+$ in methanol. Perturbation of the cavity size as well as the nature of the donor atoms on the crown ether pendants should represent a promising direction for the tuning of selective metal ion-binding in future work.

Table 6. Relative Abundances of Ion Clusters Observed in the ESI-Mass Spectrum of a Methanolic Solution Containing **2** (0.5 mM), $LiClO_4$ (0.1 mM), $NaClO_4$ (0.1 mM), and KOAc (0.1 mM)

m/*z*	ion cluster	rel abundance
378	$\{[Ru(4,4'\text{-}^tBu_2bpy)_2(dppzc)](Na)\}^{3+}$	14
555	$[Ru(4,4'\text{-}^tBu_2bpy)_2(dppzc)]^{2+}$	100
608	$\{[Ru(4,4'\text{-}^tBu_2bpy)_2(dppzc)](LiClO_4)\}^{2+}$	0.6
616	$\{[Ru(4,4'\text{-}^tBu_2bpy)_2(dppzc)](NaClO_4)\}^{2+}$	3.0
624	$\{[Ru(4,4'\text{-}^tBu_2bpy)_2(dppzc)](KClO_4)\}^{2+}$	1.7
631	$\{[Ru(4,4'\text{-}^tBu_2bpy)_2(dppzc)](LiPF_6)\}^{2+}$	1.0
639	$\{[Ru(4,4'\text{-}^tBu_2bpy)_2(dppzc)](NaPF_6)\}^{2+}$	7.0
647	$\{[Ru(4,4'\text{-}^tBu_2bpy)_2(dppzc)](KPF_6)\}^{2+}$	3.0

Acknowledgment. V.W.-W.Y. acknowledges financial support from the Research Grants Council, the Croucher Foundation and The University of Hong Kong. V.W.-M.L. acknowledges the receipt of a postgraduate studentship, administered by The University of Hong Kong.

Supporting Information Available: Text giving details of electrospray mass spectrometric experiments, a transient absorption difference spectrum generated from the laser flash photolysis of an acetonitrile solution of $[Ru(bpy)_2(dppzc)]^{2+}$ (5×10^{-5} mol dm^{-3}) and methyl viologen hexafluorophosphate (MV^{2+}, 5 mmol dm^{-3}) with 0.1 mol dm^{-3} NBu_4PF_6 as supporting electrolyte, and ESI-mass spectra showing the competitive binding of Li^+, Na^+, and K^+ ions to **2** in methanol, expanded ion clusters, and simulated isotope patterns of cation-bound species (7 pages). Ordering information is given on any current masthead page.

IC961400J

(26) Shamispur, M.; Rounaghi, G.; Popov, A. I. *J. Solution Chem.* **1980**, *9*, 701.
(27) Izatt, R. M.; Bradshaw, J. S.; Nielsen, S. A.; Lamb, J. D.; Christensen, J. J.; *Chem. Rev.* **1985**, *85*, 271.